

Arbeit zur Erlangung des akademischen Grades  
Bachelor of Science

# Flavour Mixing Effects in the Direct Detection of Dark Matter

Anja Beck  
geboren in Kempten (Allgäu)

2017

Lehrstuhl für Theoretische Physik IV  
Fakultät Physik  
Technische Universität Dortmund

Erstgutachter: Jun.-Prof. Dr. Joachim Brod  
Zweitgutachter: Prof. Dr. Heinrich Päs  
Abgabedatum: 17. Juli 2017

## Abstract

Quark flavour mixing is often neglected because of its small effects. But since dark matter only interacts weakly with baryonic matter, these tiny effects might be of importance for direct detection. This thesis examines whether flavour mixing was rightfully neglected by Altmannshofer et. al. in the discussion of a new interaction [1]. Therefore, we expand an existing framework for dark matter direct detection with the CKM mixing matrix. Thereafter, we present the new interaction, that was originally proposed to explain anomalies in the decay  $B \rightarrow K\bar{l}l$ , but also makes predictions about the direct detection of dark matter. However, when treating dark matter cross sections, this new setup ignores flavour mixing effects. Thus, we compare those new cross sections with cross sections obtained with flavour mixing and conclude that, in this case, flavour mixing was rightfully neglected.

## Kurzfassung

Die Mischung der Quark-Flavours wird in Rechnungen häufig vernachlässigt. Allerdings sind die Wechselwirkungen dunkler Materie mit baryonischer Materie sehr schwach, sodass die Effekte der Flavour-Mischung hier bedeutsam sein könnten. In dieser Arbeit wird untersucht, ob Altmannshofer et. al. die Flavour-Mischung bei der Betrachtung von direct detection unter einer neuen Wechselwirkung [1] richtigerweise nicht beachtet haben. Dazu wird zunächst ein bereits existierender Formalismus zur Berechnung von direct detection Wirkungsquerschnitten um die CKM-Mischungsmatrix erweitert. Danach wird die neue Wechselwirkung vorgestellt und der daraus resultierende Wirkungsquerschnitt für die direct detection dunkler Materie mit dem Wirkungsquerschnitt verglichen, den wird unter Berücksichtigung der Flavour-Mischung berechnen. Wir kommen zu dem Schluss, dass die Vernachlässigung der Flavour-Mischung in diesem Fall gerechtfertigt ist.



# Contents

<b>1</b>	<b>Introduction</b>	<b>1</b>
<b>2</b>	<b>The Flavour Mixing Mechanism</b>	<b>3</b>
2.1	The Higgs Mechanism . . . . .	3
2.2	Fermion Masses and Flavour Mixing . . . . .	4
<b>3</b>	<b>Introducing Flavour Mixing into an Existing Formalism</b>	<b>8</b>
3.1	Including Flavour Mixing . . . . .	9
3.2	Replacing Chiral Particle Functions . . . . .	10
3.3	Comparing Coefficients . . . . .	11
<b>4</b>	<b>The <math>L_\mu - L_\tau</math> Model</b>	<b>13</b>
4.1	The New Interaction . . . . .	13
4.2	Restrictions on the Parameter Space . . . . .	14
<b>5</b>	<b>Comparison</b>	<b>15</b>
5.1	Tree Level Interaction Cross Section . . . . .	15
5.2	Results . . . . .	16
	<b>Bibliography</b>	<b>23</b>



# 1 Introduction

Observing the movement of stars and planets is one of the earliest scientific efforts of mankind, e. g. Babylonians analysed the orbit of the Venus around 1500 BC [2]. Throughout all human civilisations, the night sky has fascinated people and will probably continue to do so, because still little is known about the particles that make up the universe. Scientists only understand about 20% of the universe's matter. They call the remaining 80% dark matter, due to its lack of luminosity. [3]

Astronomers in the 1930s found first indications of its existence. One of them was F. Zwicky, a Swiss astronomer who was interested in the Coma cluster. Through measurements of the Doppler shifts in galactic spectra, he obtained the velocity distribution and the kinetic energy of the galaxies in the cluster. Zwicky assumed that there were only gravitational interactions between the galaxies, and that he could describe them with Newtonian gravity. The virial theorem then gives the relation  $\langle T \rangle = -1/2 \langle U \rangle$  between the average kinetic energy  $\langle T \rangle$  and the average potential energy  $\langle U \rangle$ . Using this equation, Zwicky calculated the Cluster mass to be  $M_{\text{Coma}} \approx 4.5 \cdot 10^{13} M_{\text{sun}}$ . Surprisingly, this was 50 times the mass obtained by luminosity measurements. Later, a small ratio of the missing mass could be accounted for by intracluster gas, but a huge discrepancy remained and was attributed to dark matter. [3]

However, even today, after decades of intensive dark matter research, physicists do not know what dark matter particles are and how they interact. To shed light on dark matter, there currently are various detection experiments in progress around the globe, which can be classified in two categories: indirect and direct detection. Indirect detection experiments try to measure the secondary products of dark matter annihilation, whereas direct detection experiments aim at detecting the dark matter particles themselves. As shown in figure 1.1 this means the scattering of a dark matter particle off a nucleus.

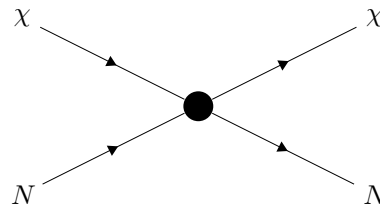


**Figure 1.1:** Direct detection: scattering of a dark matter particle  $\chi$  off a nucleus  $N$ .

Nuclei consist of protons and neutrons, which contain quarks, hence quark flavour mixing might have an effect on direct detection. In this thesis, we want to examine whether flavour mixing was rightfully neglected by Altmannshofer et. al. in their discussion of a new interaction (see publication [1]). Therefore, we first expand an existing formalism for dark matter direct detection with the CKM matrix. Secondly, we present a new interaction proposed to explain anomalies in the decay  $B \rightarrow K\bar{\ell}\ell$  that also makes predictions about the direct detection of dark matter. And finally, we compare these predictions with the direct detection cross sections that respect flavour mixing.



## 2 The Flavour Mixing Mechanism

The origins of flavour mixing go back to the 1960s, when the Italian physicist Nicola Cabibbo resolved anomalies in data of weak interactions by proposing a flavour mixing of left-handed down-type quarks. Later in 1973, Kobayaski and Maskawa extended this idea to three quark generations to explain CP violation [4]. On a mathematical level, quark flavour mixing arises from the fact that the fermion mass eigenstates do not necessarily coincide with the flavour eigenstates. In the course of this chapter, we first derive how the Higgs mechanism gives mass to particles and second take a look at fermion masses and why this leads to flavour mixing. The following calculations are based on the outlines in the textbook by Peskin and Schroeder [5, Chapter 20] and the theoretical discussion of CP violation in [6, Chapter 1.2.1].

### 2.1 The Higgs Mechanism

We consider a complex scalar field  $\Phi$  that interacts with itself through a potential

$$V(\Phi) = -\mu^2 \Phi^\dagger \Phi + \frac{\lambda}{2} (\Phi^\dagger \Phi)^2, \quad \mu^2 > 0.$$

If  $\lambda > 0$  and  $\Phi$  is a singlet, this potential has two minima, which occur at

$$\langle \Phi \rangle = \pm \sqrt{\frac{\mu^2}{\lambda}}. \quad (2.1)$$

These are the vacuum expectation values of  $\Phi$ .

To show how symmetry breaking leads to massive particles, we now introduce a symmetry, for example  $SU(2)$ , coupled to  $\Phi$ . In order to couple to  $SU(2)$ ,  $\Phi$  has to be a doublet  $(\Phi_1, \Phi_2)$  with covariant derivative

$$D_\mu \Phi = (\partial_\mu - ig \sum_{a=1}^3 A_\mu^a \tau^a) \Phi,$$

## 2 The Flavour Mixing Mechanism

---

where the  $\tau^a$  are the generators of  $SU(2)$ . Since condition (2.1) still holds for the absolute value of  $\Phi$ , there now is an infinite number of vacuum expectation values, arranged in a circle. We are free to choose one and make the simple choice

$$\langle \Phi \rangle = \frac{1}{\sqrt{2}} \begin{pmatrix} 0 \\ v \end{pmatrix}, \quad v = \sqrt{\frac{2\mu^2}{\lambda}}. \quad (2.2)$$

The kinetic energy of  $\Phi$  is then

$$\begin{aligned} (D_\mu \Phi)^2 &= \frac{1}{2} (\partial_\mu v) (\partial^\mu v) \\ &\quad - ig (\partial^\mu \begin{pmatrix} 0 \\ v \end{pmatrix}) \left( \sum_{a=1}^3 A_\mu^a \tau^a \begin{pmatrix} 0 \\ v \end{pmatrix} \right) \\ &\quad - \frac{1}{2} g^2 \begin{pmatrix} 0 \\ v \end{pmatrix} \sum_{a,b=1}^3 \tau^a \tau^b \begin{pmatrix} 0 \\ v \end{pmatrix} A_\mu^a A^{b\mu}. \end{aligned} \quad (2.3)$$

Using the anticommutator  $\{\tau^a, \tau^b\} = \delta_{ab}/2$ , we can simplify the last expression in (2.3) to

$$-\frac{1}{2} g^2 \begin{pmatrix} 0 \\ v \end{pmatrix} \sum_{a,b=1}^3 \tau^a \tau^b \begin{pmatrix} 0 \\ v \end{pmatrix} A_\mu^a A^{b\mu} = -\frac{g^2 v^2}{8} \sum_{a=1}^3 A_\mu^a A^{a\mu},$$

which is a mass term  $\mathcal{L}_m = -\frac{1}{2} m_A^2 A_\mu A^\mu$  that assigns the mass  $m_A = gv/2$  to all three gauge bosons that are needed in a  $SU(2)$  symmetry. By expanding the system with an additional  $U(1)$  symmetry, the kinetic energy would again provide three gauge boson masses, leaving the fourth gauge boson massless. The massive bosons can be identified as  $W^\pm, Z^0$ , and the massless one as the photon.

The scalar field  $\Phi$  that gives mass to the gauge bosons of a  $SU(2) \times U(1)$  symmetry is usually called Higgs boson. Obtaining particle mass terms in the kinetic energy of the Higgs, is, unsurprisingly, referred to as the Higgs mechanism.

## 2.2 Fermion Masses and Flavour Mixing

Hereafter, we describe how the standard model fermions get their masses and how this leads to quark flavour mixing. But beforehand, we introduce the notation used in this and the following chapters. The leptons and quark chiral particle multiplets

are

$$\begin{aligned}
 E_R &= (e_R, \mu_R, \tau_R) , & Y_E &= -2 ; \\
 L_L &= \left( \begin{pmatrix} \nu_e \\ e \end{pmatrix}_L, \begin{pmatrix} \nu_\mu \\ \mu \end{pmatrix}_L, \begin{pmatrix} \nu_\tau \\ \tau \end{pmatrix}_L \right) , & Y_L &= -1 ; \\
 U_R &= (u_R, c_R, t_R) , & Y_U &= \frac{4}{3} ; \\
 D_R &= (d_R, s_R, b_R) , & Y_D &= -\frac{2}{3} ; \\
 Q_L &= \left( \begin{pmatrix} u \\ d \end{pmatrix}_L, \begin{pmatrix} c \\ s \end{pmatrix}_L, \begin{pmatrix} t \\ b \end{pmatrix}_L \right) , & Y_Q &= \frac{1}{3} ;
 \end{aligned}$$

where the hypercharge  $Y$  is given. It is related to the electric charge  $Q$  and the third component of the weak isospin  $I_3$  through the Gell-Mann-Nishijima formula [4, Chapter 10.7]

$$Q = \frac{Y}{2} + I_3 .$$

The right-handed particles are singlets under  $SU(2)$  and therefore  $I_3^{(r.h.)} = 0$ . We later also use the left-handed components  $E_L = (e_L, \mu_L, \tau_L)$ ,  $D_L = (d_L, s_L, b_L)$ , and  $U_L = (u_L, c_L, t_L)$ .

The electroweak interaction lagrangian for the standard model fermions is

$$\begin{aligned}
 \mathcal{L}^{(\text{int})} &= \bar{E}_R \gamma^\mu (i\partial_\mu - g_1 Y_E B_\mu) E_R + \bar{L}_L \gamma^\mu (i\partial_\mu - g_1 Y_L B_\mu - g_2 \sum_{a=1}^3 A_\mu^a \tau^a) L_L \\
 &+ \bar{D}_R \gamma^\mu (i\partial_\mu - g_1 Y_D B_\mu) D_R + \bar{U}_R \gamma^\mu (i\partial_\mu - g_1 Y_U B_\mu) U_R \\
 &+ \bar{Q}_L \gamma^\mu (i\partial_\mu - g_1 Y_Q B_\mu - g_2 \sum_{a=1}^3 A_\mu^a \tau^a) Q_L ,
 \end{aligned} \tag{2.4}$$

where  $B_\mu, A_\mu^a$  are the gauge bosons corresponding to  $U(1)_Y \times SU(2)$ . The coupling constants are  $g_1$  and  $g_2$ , and the  $\tau^a$  are again the  $SU(2)$  generators. This lagrangian describes massless particles. In order to get a fermion mass term, one has to couple the left- and right-handed part of a particle. Since a direct coupling between a  $SU(2)$  singlet and a  $SU(2)$  doublet violates gauge invariance, a connecting field is necessary. To preserve invariance under Lorentz,  $U(1)_Y$ , and  $SU(2)$  transformations, this field must have spin 0, hypercharge  $Y = 1/2$ , and be a doublet. We identify this field with  $\Phi$  from the previous chapter and write down the mass terms for the fermions

$$\mathcal{L}^{(\text{mass})} = - [\bar{L}_L \Phi \lambda^e E_R + \bar{Q}_L \Phi \lambda^d D_R + \bar{Q}_L i \sigma^2 \Phi^\dagger \lambda^u U_R + \text{h. c.}] ,$$

## 2 The Flavour Mixing Mechanism

---

with complex matrix coupling constants  $\lambda^e, \lambda^d, \lambda^u$ . Replacing  $\Phi$  with its vacuum expectation value (2.2) gives

$$\mathcal{L}^{(\text{mass})} = -\frac{v}{\sqrt{2}} [\bar{E}_L \lambda^e E_R + \bar{D}_L \lambda^d D_R + \bar{U}_L \lambda^u U_R + \text{h. c.}] . \quad (2.5)$$

The interaction lagrangian  $\mathcal{L}^{(\text{int})}$  (see (2.4)) is invariant under the unitary transformations

$$\begin{aligned} E_L &\rightarrow S_e E_L , & E_R &\rightarrow R_e E_R , \\ U_L &\rightarrow S_u U_L , & U_R &\rightarrow R_u U_R , \\ D_L &\rightarrow S_d D_L , & D_R &\rightarrow R_d D_R . \end{aligned}$$

Thus, we can diagonalize the interactions in (2.5), using these transformations. The diagonal lepton coupling is  $\tilde{\lambda}^e = S_e \lambda^e R_e^\dagger$  and parametrizes the lepton masses

$$m_e = \frac{v}{\sqrt{2}} \tilde{\lambda}_{11}^e , \quad m_\mu = \frac{v}{\sqrt{2}} \tilde{\lambda}_{22}^e , \quad m_\tau = \frac{v}{\sqrt{2}} \tilde{\lambda}_{33}^e .$$

The diagonal coupling for up-type quarks is  $\tilde{\lambda}^u = S_u \lambda^u R_u^\dagger$ , giving the corresponding masses

$$m_u = \frac{v}{\sqrt{2}} \tilde{\lambda}_{11}^u , \quad m_c = \frac{v}{\sqrt{2}} \tilde{\lambda}_{22}^u , \quad m_t = \frac{v}{\sqrt{2}} \tilde{\lambda}_{33}^u .$$

The transformed coupling of the down-type quarks is  $\tilde{\lambda}^d = S_d \lambda^d R_d^\dagger$ , leading to the down-type masses

$$m_d = \frac{v}{\sqrt{2}} \tilde{\lambda}_{11}^d , \quad m_s = \frac{v}{\sqrt{2}} \tilde{\lambda}_{22}^d , \quad m_b = \frac{v}{\sqrt{2}} \tilde{\lambda}_{33}^d .$$

The transformed particle multiplets are now mass eigenstates. But when looking at couplings of up- and down-type quarks, e. g. the current

$$\bar{U}_L \gamma^\mu D_L ,$$

the unitary transformations change the interaction to

$$\bar{U}_L \gamma^\mu S_u^\dagger S_d D_L ,$$

where we identify the CKM matrix  $V = S_u^\dagger S_d$ . Because  $S_u, S_d$  are already determined by the diagonalizations above, the CKM matrix is not equal to the identity

matrix in general. In fact,  $V$  alters left-handed currents measurably. The most recent data by the Particle Data Group determines the parameters of the Wolfenstein parametrization

$$V = \begin{pmatrix} 1 - \frac{\lambda^2}{2} & \lambda & A\lambda^3(\rho - i\eta) \\ -\lambda & 1 - \frac{\lambda^2}{2} & A\lambda^2 \\ A\lambda^3(1 - \rho - i\eta) & -A\lambda^2 & 1 \end{pmatrix} + \mathcal{O}(\lambda^4)$$

to be (see [7, Chapter 12]<sup>1</sup>)

$$\begin{aligned} \lambda &= 0.224\,96 \pm 0.000\,48 \, , & A &= 0.823 \pm 0.013 \, , \\ \rho &= 0.141 \pm 0.019 \, , & \eta &= 0.349 \pm 0.012 \, . \end{aligned} \quad (2.6)$$

---

<sup>1</sup>The Particle Data Group actually suggests two different sets of parameters obtained by two different methods. We choose one arbitrarily, because they only differ in the second decimal position, which does not make any difference in our calculations later.

### 3 Introducing Flavour Mixing into an Existing Formalism

In this chapter we incorporate flavour mixing into an existing formalism. We use the model described in [8]. It provides a framework to calculate cross sections for the direct detection of dark matter. The model is based on a set of dimension-five, -six, and -seven operators. We restrict our calculations to the dimension-six operators, which are

$$\begin{aligned} R_{1,q} &= (\bar{\chi}_0 \gamma_\mu \chi_0) (\bar{q} \gamma^\mu q) , & R_{3,q} &= (\bar{\chi}_0 \gamma_\mu \chi_0) (\bar{q} \gamma^\mu \gamma_5 q) , \\ R_{2,q} &= (\bar{\chi}_0 \gamma_\mu \gamma_5 \chi_0) (\bar{q} \gamma^\mu q) , & R_{4,q} &= (\bar{\chi}_0 \gamma_\mu \gamma_5 \chi_0) (\bar{q} \gamma^\mu \gamma_5 q) . \end{aligned} \quad (3.1)$$

Here  $q = (u, d, c, s, t, b)$  is a quark and  $\chi_0$  is the component of the weak dark matter multiplet that has no electric charge.

Since the CKM mixing only applies to the left-handed down-type quarks, we need to rewrite these operators in terms of the left- and righthanded particle multiplets to include the CKM matrix. These chiral operators are

$$\begin{aligned} Q_{1ij} &= (\bar{\chi} \gamma_\mu \tilde{\tau}^a \chi) (\bar{Q}_L^i \gamma^\mu \tau^a Q_L^j) , & Q_{5ij} &= (\bar{\chi} \gamma_\mu \gamma_5 \tilde{\tau}^a \chi) (\bar{Q}_L^i \gamma^\mu \tau^a Q_L^j) , \\ Q_{2ij} &= (\bar{\chi} \gamma_\mu \chi) (\bar{Q}_L^i \gamma^\mu Q_L^j) , & Q_{6ij} &= (\bar{\chi} \gamma_\mu \gamma_5 \chi) (\bar{Q}_L^i \gamma^\mu Q_L^j) , \\ Q_{3ij} &= (\bar{\chi} \gamma_\mu \chi) (\bar{U}_R^i \gamma^\mu U_R^j) , & Q_{7ij} &= (\bar{\chi} \gamma_\mu \gamma_5 \chi) (\bar{U}_R^i \gamma^\mu U_R^j) , \\ Q_{4ij} &= (\bar{\chi} \gamma_\mu \chi) (\bar{D}_R^i \gamma^\mu D_R^j) , & Q_{8ij} &= (\bar{\chi} \gamma_\mu \gamma_5 \chi) (\bar{D}_R^i \gamma^\mu D_R^j) . \end{aligned} \quad (3.2)$$

The operators  $\tilde{\tau}^a$  and  $\tau^a$  are the generators of  $SU(2)$  in the corresponding spin-representation. The left-handed quarks come in doublets, therefore the generators are the Pauli matrices  $\sigma_a$ :

$$\tau^a = \frac{\sigma_a}{2} .$$

Since the size of the dark matter multiplet is unknown, we use the general spin-representation

$$\begin{aligned} (\tilde{\tau}^1 \pm i \tilde{\tau}^2)_{\sigma' \sigma} &= \delta_{\sigma' \sigma \pm 1} \sqrt{(j \mp \sigma)(j \pm \sigma + 1)} , \\ \tilde{\tau}_{\sigma' \sigma}^3 &= \sigma \delta_{\sigma' \sigma} , \end{aligned}$$

where  $j$  is the spin value with  $-j \leq \sigma \leq j$  and  $-j \leq \sigma' \leq j$ . However, we only keep the electrically uncharged component  $\chi_0$  of the multiplet.

In the following sections, we go through the steps of including the CKM matrix in the formalism:

1. Incorporation of flavour mixing by replacing the pure left-handed down-type quarks with the mixed quarks.
2. Rewriting the chiral particle multiplets in terms of the unchiral particle multiplets and projection operators.
3. Writing down the interaction lagrangian in terms of the operators in (3.1) and (3.2) separately, and then comparing the coefficients.

### 3.1 Including Flavour Mixing

The inclusion of the CKM matrix only affects the chiral operators with left-handed quarks:  $Q_{1ij}, Q_{2ij}, Q_{5ij}, Q_{6ij}$ . Since the dark matter part of the interaction remains unchanged, we only look at the quark part of the interaction, which becomes

$$\begin{aligned}\bar{Q}_L^i \gamma^\mu \tau^a Q_L^j &= \begin{pmatrix} \bar{u}_L^i \\ \bar{d}_L^i \end{pmatrix} \gamma^\mu \begin{pmatrix} u_L^j \\ d_L^j \end{pmatrix} = \frac{1}{2} \bar{u}_L^i \gamma^\mu \sigma_a d_L^j + \frac{1}{2} \bar{d}_L^i \gamma^\mu \sigma_a d_L^j \\ &= \frac{1}{2} \bar{u}_L^i \gamma^\mu \sigma_a u_L^j + \frac{1}{2} (V_{id}^* \bar{d}_L + V_{is}^* \bar{s}_L + V_{ib}^* \bar{b}_L) \gamma^\mu \sigma_a (V_{jd} d_L + V_{js} s_L + V_{jb} b_L)\end{aligned}$$

for  $Q_{1ij}, Q_{5ij}$  and

$$\begin{aligned}\bar{Q}_L^i \gamma^\mu Q_L^j &= \begin{pmatrix} \bar{u}_L^i \\ \bar{d}_L^i \end{pmatrix} \gamma^\mu \begin{pmatrix} u_L^j \\ d_L^j \end{pmatrix} = \bar{u}_L^i \gamma^\mu d_L^j + \bar{d}_L^i \gamma^\mu d_L^j \\ &= \bar{u}_L^i \gamma^\mu u_L^j + (V_{id}^* \bar{d}_L + V_{is}^* \bar{s}_L + V_{ib}^* \bar{b}_L) \gamma^\mu (V_{jd} d_L + V_{js} s_L + V_{jb} b_L)\end{aligned}$$

for  $Q_{2ij}, Q_{6ij}$ . For simplicity, we only keep the light quarks  $u, d, s$  and neglect mixed terms. So the whole set of quark interactions is

$$\begin{aligned}\bar{Q}_L^i \gamma^\mu \tau^a Q_L^j &\approx \frac{1}{2} \bar{u}_L \gamma^\mu u_L \delta_{ij} \delta_{iu} \delta_{a3} - \frac{1}{2} \delta_{a3} (V_{id}^* V_{jd} \bar{d}_L \gamma^\mu d_L + V_{is}^* V_{js} \bar{s}_L \gamma^\mu s_L) , \\ \bar{Q}_L^i \gamma^\mu Q_L^j &\approx \bar{u}_L \gamma^\mu u_L \delta_{ij} \delta_{iu} + V_{id}^* V_{jd} \bar{d}_L \gamma^\mu d_L + V_{is}^* V_{js} \bar{s}_L \gamma^\mu s_L , \\ \bar{u}_R^i \gamma^\mu u_R^j &\approx \bar{u}_R \gamma^\mu u_R \delta_{ij} \delta_{iu} , \\ \bar{d}_R^i \gamma^\mu d_R^j &\approx \bar{d}_R \gamma^\mu d_R \delta_{ij} \delta_{id} + \bar{s}_R \gamma^\mu s_R \delta_{ij} \delta_{is} .\end{aligned}$$

Note that, by only keeping diagonal interactions, we abolish the expressions including  $\tau^1, \tau^2$ , respectively  $\tilde{\tau}^1, \tilde{\tau}^2$ . Therefore, the dark matter part of the interactions  $Q_{1ij}, Q_{5ij}$  becomes

$$\begin{aligned}\bar{\chi}\gamma_\mu\tilde{\tau}^3\chi &= \sigma^0\bar{\chi}_0\gamma_\mu\chi_0, \\ \bar{\chi}\gamma_\mu\gamma_5\tilde{\tau}^3\chi &= \sigma^0\bar{\chi}_0\gamma_\mu\gamma_5\chi_0,\end{aligned}$$

because, as mentioned before, we are only interested in the electrically uncharged component  $\chi_0$  of  $\chi$ .

### 3.2 Replacing Chiral Particle Functions

The next step is rewriting the chiral particle multiplets in terms of the unchiral particle multiplets using the projection operators  $P_L, P_R$ . This leads to

$$\begin{aligned}\bar{Q}_L^i\gamma^\mu\tau^a Q_L^j &= \frac{1}{4}(\bar{u}\gamma^\mu u\delta_{ij}\delta_{iu}\delta_{3a} - V_{id}^*V_{jd}\bar{d}\gamma^\mu d\delta_{3a} - V_{is}^*V_{js}\bar{s}\gamma^\mu s\delta_{3a}) \\ &\quad - \frac{1}{4}(\bar{u}\gamma^\mu\gamma_5 u\delta_{ij}\delta_{iu}\delta_{3a} - V_{id}^*V_{jd}\bar{d}\gamma^\mu\gamma_5 d\delta_{3a} - V_{is}^*V_{js}\bar{s}\gamma^\mu\gamma_5 s\delta_{3a}), \\ \bar{Q}_L^i\gamma^\mu Q_L^j &= \frac{1}{2}(\bar{u}\gamma^\mu u\delta_{iu}\delta_{ij} + V_{id}^*V_{jd}\bar{d}\gamma^\mu d + V_{is}^*V_{js}\bar{s}\gamma^\mu s) \\ &\quad - \frac{1}{2}(\bar{u}\gamma^\mu\gamma_5 u\delta_{iu}\delta_{ij} + V_{id}^*V_{jd}\bar{d}\gamma^\mu\gamma_5 d + V_{is}^*V_{js}\bar{s}\gamma^\mu\gamma_5 s), \\ \bar{u}_R^i\gamma^\mu u_R^j &= \frac{1}{2}(\bar{u}\gamma^\mu u\delta_{ij}\delta_{iu} + \bar{u}\gamma^\mu\gamma_5 u\delta_{ij}\delta_{iu}), \\ \bar{d}_R^i\gamma^\mu d_R^j &= \frac{1}{2}(\bar{d}\gamma^\mu d\delta_{ij}\delta_{id} + \bar{d}\gamma^\mu\gamma_5 d\delta_{ij}\delta_{id} + \bar{s}\gamma^\mu s\delta_{ij}\delta_{is} + \bar{s}\gamma^\mu\gamma_5 s\delta_{ij}\delta_{is}).\end{aligned}$$

At this point we can express the chiral operators in terms of the original operators from (3.1):

$$\begin{aligned}Q_{1ij} &= \frac{\delta_{3a}\sigma^0}{4}(R_{1u}\delta_{ij}\delta_{iu} - V_{id}^*V_{jd}R_{1d} - V_{is}^*V_{js}R_{1s}) \\ &\quad - \frac{\delta_{3a}\sigma^0}{4}(R_{3u}\delta_{ij}\delta_{iu} - V_{id}^*V_{jd}R_{3d} - V_{is}^*V_{js}R_{3s}), \\ Q_{2ij} &= \frac{1}{2}(R_{1u}\delta_{iu}\delta_{ij} + V_{id}^*V_{jd}R_{1d} + V_{is}^*V_{js}R_{1s}) \\ &\quad - \frac{1}{2}(R_{3u}\delta_{iu}\delta_{ij} + V_{id}^*V_{jd}R_{3d} + V_{is}^*V_{js}R_{3s}), \\ Q_{3ij} &= \frac{1}{2}(R_{1u}\delta_{ij}\delta_{iu} + R_{3u}\delta_{ij}\delta_{iu}), \\ Q_{4ij} &= \frac{1}{2}(R_{1d}\delta_{ij}\delta_{id} + R_{3d}\delta_{ij}\delta_{id} + R_{1s}\delta_{ij}\delta_{is} + R_{3s}\delta_{ij}\delta_{is}).\end{aligned}\tag{3.3}$$



The operators  $Q_{5ij} - Q_{8ij}$  can be obtained from  $Q_{1ij} - Q_{4ij}$  by replacing  $R_{1q}$  with  $R_{2q}$  and  $R_{3q}$  with  $R_{4q}$ .

### 3.3 Comparing Coefficients

Our final step is expressing the coefficients  $K_{l,q}$  of the original operators  $R_{l,q}$  in (3.1) in terms of the coefficients  $C_{lij}$  of the chiral operators  $Q_{lij}$  in (3.2). To get there, we look at the overall interaction. The interaction cannot depend on the choice of particle representation (chiral or non-chiral), therefore

$$\sum_{l,q} K_{l,q} R_{l,q} \stackrel{!}{=} \sum_{l,i,j} C_{lij} Q_{lij} . \quad (3.4)$$

We put the interactions (3.3) into the right-hand side of equation (3.4) and rearrange the expression in terms of the  $R_{l,q}$ . By concluding that  $K_{l,q}$  on the left-hand side must be equal to the terms in front of  $R_{l,q}$  on the right-hand side, we get the dependencies

$$\begin{aligned} K_{1,u} &= \sum_{i,j} \frac{\delta_{ij} \delta_{iu}}{2} \left( C_{1ij} \frac{\delta_{3a} \sigma^0}{2} + C_{2ij} + C_{3ij} \right) , \\ K_{1,d} &= \sum_{i,j} \frac{1}{2} \left( -V_{id}^* V_{jd} C_{1ij} \frac{\delta_{3a} \sigma^0}{2} + V_{id}^* V_{jd} C_{2ij} + \delta_{ij} \delta_{id} C_{4ij} \right) , \\ K_{1,s} &= \sum_{i,j} \frac{1}{2} \left( -V_{is}^* V_{js} C_{1ij} \frac{\delta_{3a} \sigma^0}{2} + V_{is}^* V_{js} C_{2ij} + \delta_{ij} \delta_{is} C_{4ij} \right) , \\ K_{2,u} &= \sum_{i,j} \frac{\delta_{ij} \delta_{iu}}{2} \left( \frac{\delta_{3a} \sigma^0}{2} C_{5ij} + C_{6ij} + C_{7ij} \right) , \\ K_{2,d} &= \sum_{i,j} \frac{1}{2} \left( -V_{id}^* V_{jd} \frac{\delta_{3a} \sigma^0}{2} C_{5ij} + C_{6ij} V_{id}^* V_{jd} + \delta_{ij} \delta_{id} C_{8ij} \right) , \\ K_{2,s} &= \sum_{i,j} \frac{1}{2} \left( -V_{is}^* V_{js} \frac{\delta_{3a} \sigma^0}{2} C_{5ij} + C_{6ij} V_{is}^* V_{js} + \delta_{ij} \delta_{is} C_{8ij} \right) , \\ K_{3,u} &= \sum_{i,j} \frac{\delta_{ij} \delta_{iu}}{2} \left( -C_{1ij} \frac{\delta_{3a} \sigma^0}{2} - C_{2ij} + C_{3ij} \right) , \\ K_{3,d} &= \sum_{i,j} \frac{1}{2} \left( C_{1ij} \frac{\delta_{3a} \sigma^0}{2} V_{id}^* V_{jd} - V_{id}^* V_{jd} C_{2ij} + \delta_{ij} \delta_{id} C_{4ij} \right) , \\ K_{3,s} &= \sum_{i,j} \frac{1}{2} \left( C_{1ij} \frac{\delta_{3a} \sigma^0}{2} V_{is}^* V_{js} - V_{is}^* V_{js} C_{2ij} + \delta_{ij} \delta_{is} C_{4ij} \right) , \end{aligned}$$

$$\begin{aligned}
K_{4,u} &= \sum_{i,j} \frac{\delta_{ij}\delta_{iu}}{2} \left( -\frac{\delta_{3a}\sigma^0}{2} C_{5ij} - C_{6ij} + C_{7ij} \right) , \\
K_{4,d} &= \sum_{i,j} \frac{1}{2} \left( \frac{\delta_{3a}\sigma^0}{2} C_{5ij} V_{id}^* V_{jd} - C_{6ij} V_{id}^* V_{jd} + \delta_{ij}\delta_{id} C_{8ij} \right) , \\
K_{4,s} &= \sum_{i,j} \frac{1}{2} \left( \frac{\delta_{3a}\sigma^0}{2} C_{5ij} V_{is}^* V_{js} - C_{6ij} V_{is}^* V_{js} + \delta_{ij}\delta_{is} C_{8ij} \right) . \quad (3.5)
\end{aligned}$$

To obtain a hermitian interaction, the coefficients need to fulfil the relation  $C_{lij} = C_{lji}^*$ .

## 4 The $L_\mu - L_\tau$ Model

In this chapter, we present a proposed extension to the standard model by Altmannshofer et. al. in publication [9]. The authors originally aimed at explaining anomalies in the decay  $B \rightarrow K\ell\bar{\ell}$ , but also obtained predictions for the direct detection of dark matter in the succeeding publication [1]. We will later compare their results with the formalism in the previous chapter that includes the CKM mixing.

### 4.1 The New Interaction

The aforementioned extension to the standard model consists of a new  $U(1)'$  gauge group. The related vector-boson is called  $Z'$ , and it couples to the muon and tau lepton families, and a new set of vector-like quarks  $U, D, Q$ . The standard model quarks indirectly couple to the  $Z'$  as well, since they mix with the new quarks through a Yukawa coupling:

$$\begin{aligned}\mathcal{L}^{(\text{mix})} = & \Phi' \bar{\tilde{D}}_R (Y_{Qb} b_L + Y_{Qs} s_L + Y_{Qd} d_L) \\ & + \Phi' \bar{\tilde{U}}_R (Y_{Qt} t_L + Y_{Qc} c_L + Y_{Qu} u_L) \\ & + \Phi'^\dagger \tilde{U}_L (Y_{Ut} t_R + Y_{Uc} c_R + Y_{Uu} u_R) \\ & + \Phi'^\dagger \tilde{D}_L (Y_{Db} b_R + Y_{Ds} s_R + Y_{Dd} d_R) + \text{h. c.} ,\end{aligned}$$

where  $\tilde{Q}_R = (\tilde{U}_R, \tilde{D}_R)$ ,  $Q_L = (U_L, D_L)$  are the weak doublets,  $Y_{ij}$  are the coupling constants, and  $\Phi'$  is a Higgs-like field that gives mass to the  $Z'$ .

In publication [1], a coupling to a dark matter fermion  $\chi$  is additionally established. The interaction lagrangian then is:

$$\begin{aligned}\mathcal{L}_{Z'}^{(\text{int})} = & g' Z'_\alpha \times q_l (\bar{L}_L^2 \gamma^\alpha L_L^2 - \bar{L}_L^3 \gamma^\alpha L_L^3 + \bar{\mu}_R \gamma^\alpha \mu_R - \bar{\tau}_R \gamma^\alpha \tau_R) \\ & + g' Z'_\alpha \times v_{\Phi'}^2 \sum_{i,j}^3 \left( -\frac{Y_{Di} Y_{Dj}^*}{2m_D^2} \bar{D}_R^i \gamma^\alpha D_R^j - \frac{Y_{Ui} Y_{Uj}^*}{2m_U^2} \bar{U}_R^i \gamma^\alpha U_R^j + \frac{Y_{Qi} Y_{Qj}^*}{2m_Q^2} \bar{Q}_L^i \gamma^\alpha Q_L^j \right) \\ & + g' Z'_\alpha \times q_\chi (\bar{\chi} \gamma^\alpha \chi) ,\end{aligned}$$

where  $q_l, q_\chi$  are the  $U(1)'$  charges of the leptons and the dark matter particle,  $m_{U,D,Q}$  are the masses of the new quarks, and  $v_{\Phi'}$  is the vacuum expectation value of  $\Phi'$ .

## 4.2 Restrictions on the Parameter Space

In [1], Altmannshofer et. al. discuss restrictions on the parameter space arising from the  $B$  decay mentioned above, dark matter relic density and direct detection limits. They find that experimental data from  $B \rightarrow K \bar{l} l$  limits the ratio of the  $Z'$  mass  $m_{Z'}$  and the coupling  $g'$  to

$$540 \text{ GeV} \lesssim \frac{m_{Z'}}{g'} \lesssim 4.9 \text{ TeV} , \quad (4.1)$$

with  $m_{Z'} \gtrsim 10 \text{ GeV}$ .

Regarding dark matter relic density, they conclude that only

$$m_{Z'} \approx 2m_\chi , \quad (4.2)$$

with the dark matter mass  $m_\chi$ , leads to correct results. Since they neglect flavour mixing in the nucleus, direct detection has to occur through the loop diagram in Figure 4.1. The corresponding nucleon cross section at zero momentum transfer is

$$\sigma_{0,\text{loop}} = \frac{\mu_{A\chi}^2}{A^2 \pi} \left( \frac{\alpha_{em} Z}{3\pi} \frac{g'^2 q_\chi q_l}{m_{Z'}^2} \log \left( \frac{m_\mu^2}{m_\tau^2} \right) \right)^2 , \quad (4.3)$$

where  $\mu_{A\chi}$  is the reduced mass of the nucleus and the dark matter particle  $\chi$ , and  $A, Z$  are the nucleon and proton numbers.

When discussing limits to the parameter space, they distinguish two cases. For  $q_l = q_\chi = 1$ , experimental data favours the parameter region

$$\begin{aligned} 10 \text{ GeV} &\lesssim m_{Z'} \lesssim 46 \text{ GeV} , \\ 2 \cdot 10^{-3} &\lesssim g' \lesssim 10^{-2} , \end{aligned} \quad (4.4)$$

leaving possible dark matter masses in the range  $(5 - 23) \text{ GeV}$ . For  $q_l = 1, q_\chi = 1/6$  no further restrictions of the parameters can be found.

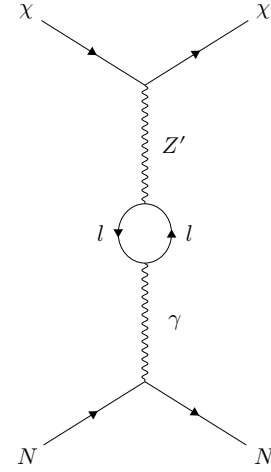


**Figure 4.1:** Direct detection loop diagram as proposed in [1].

## 5 Comparison

We now assume that only  $b, s, \mu, \tau$  and dark matter particles couple to  $Z'$ , and dark matter couples exclusively to  $Z'$ . Taking into account flavour mixing, a tree level interaction of dark matter particles and nucleons is then possible. We take a look at this option in the first of the following sections. Afterwards, we compare the direct detection cross sections of the tree level interaction and the loop interaction.

### 5.1 Tree Level Interaction Cross Section

If we assume flavour mixing to be of importance, a dark matter particle can interact with the strange and bottom parts of a down quark in a nucleus through the tree level diagram shown in Figure 5.1. In terms of the operators in (3.2), the diagram corresponds to  $Q_{2bs}, Q_{2sb}$ . The related coefficients are

$$C_{2bs} = C_{2sb}^* = q_\chi \frac{Y_{Qb} Y_{Qs}^*}{2m_Q^2} ,$$

for which [9] gives an approximation of

$$\text{Re}(C_{2bs}) \approx 8 \cdot 10^{-10} \text{ GeV}^{-2} . \quad (5.1)$$

By using equations (3.5), we obtain

$$\begin{aligned} K_{1,d} &= +\text{Re}(V_{cd}^* V_{td} C_{2sb}) , \\ K_{1,s} &= +\text{Re}(V_{cs}^* V_{ts} C_{2sb}) , \\ K_{3,d} &= -\text{Re}(V_{cd}^* V_{td} C_{2sb}) , \\ K_{3,s} &= -\text{Re}(V_{cs}^* V_{ts} C_{2sb}) . \end{aligned}$$

These are the coefficients of the spin-independent interaction  $R_{1,q} = (\bar{\chi} \gamma^\mu \chi)(\bar{q} \gamma_\mu q)$  and the spin-dependent interaction  $R_{3,q} = (\bar{\chi} \gamma^\mu \chi)(\bar{q} \gamma_\mu \gamma_5 q)$ . We neglect the latter, because it is several orders of magnitude smaller than the spin-independent cross section. However, there is no interaction with strange quarks, as they are only available as sea quarks. Thus, we are left with the spin-independent vector interaction

$$\mathcal{L} = K_{1,d} (\bar{\chi} \gamma^\mu \chi) (\bar{d} \gamma_\mu d) .$$

As explained by [10, Chapter 7], this operator counts the number of down quarks. So the nucleon cross section at zero momentum transfer is

$$\sigma_{0,\text{tree}} = \frac{\mu_{A\chi}^2}{A^2\pi} |ZC_p + (A - Z)C_n|^2, \quad (5.2)$$

where  $C_p = K_{1,d}$  and  $C_n = 2K_{1,d}$  are the proton and neutron coefficients.

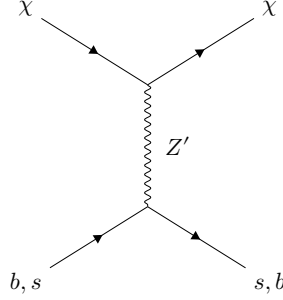


**Figure 5.1:** Tree level diagram for direct detection through exchange of a  $Z'$  boson.

## 5.2 Results

We now compare the nucleon cross sections for the loop interaction  $\sigma_{0,\text{loop}}$  (see equation (4.3) and Figure 4.1) and the tree level interaction  $\sigma_{0,\text{tree}}$  (see equation (5.2) and Figure 5.1). We choose Xenon, which is used in the LUX and XENON100 experiments, as detection material. The most abundant isotope is Xenon-129, therefore  $Z = 54$ ,  $A = 129$  [11]. For the CKM matrix elements we use the values given in (2.6).

In the following, we show various plots, in which we follow Altmannshofer et. al. with their distinction of the cases  $q_\chi = 1$  and  $q_\chi = 1/6$  in [1]. Keep in mind that for the former the dark matter mass cannot be much larger than 23 GeV, but for the latter no restriction is made. Therefore, we choose different scales for the dark matter mass in the plots. The green shaded area always corresponds to  $\sigma_{0,\text{loop}}$ , whereas the lines visualize  $\sigma_{0,\text{tree}}$ .

First, we consider the bound in equation (4.1) for  $\sigma_{0,\text{loop}}$ . Figure 5.2 shows  $\sigma_{0,\text{loop}}$  (shaded green) within this bound and  $\sigma_{0,\text{tree}}$  with various choices for  $C_{2bs} = C$  that are in accordance with (5.1). But even for quite large values of  $C_{2bs}$ , the tree level cross section cannot reach the loop cross section. This is a strong hint that

Altmannshofer et. al. correctly neglected CKM mixing in their predictions for dark matter direct detection.

Since there are no restrictions concerning the imaginary part of  $C_{2bs}$ , we enlarged  $\text{Im}(C_{2bs})$  until we reached  $\sigma_{0,\text{loop}}$  in Figure 5.3. But this can only be achieved by choosing imaginary parts two orders of magnitude larger than the real part of  $C_{2bs}$ . Even though this is possible, we consider an imaginary part of this magnitude to be very odd.

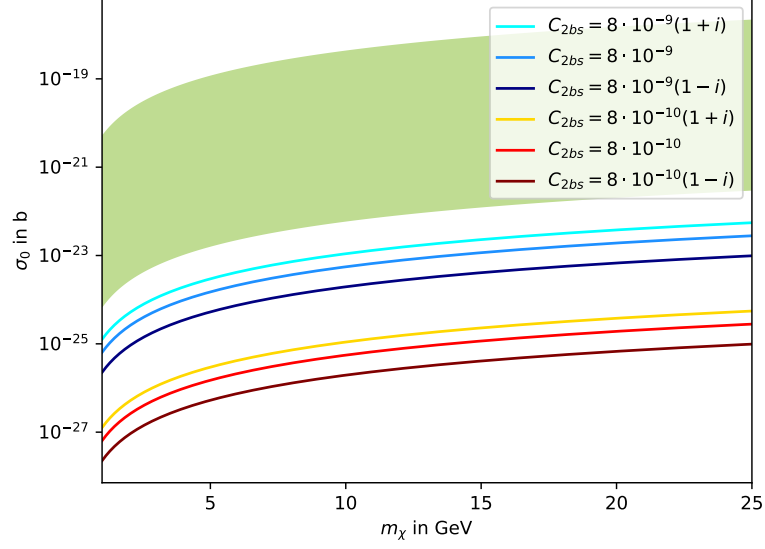
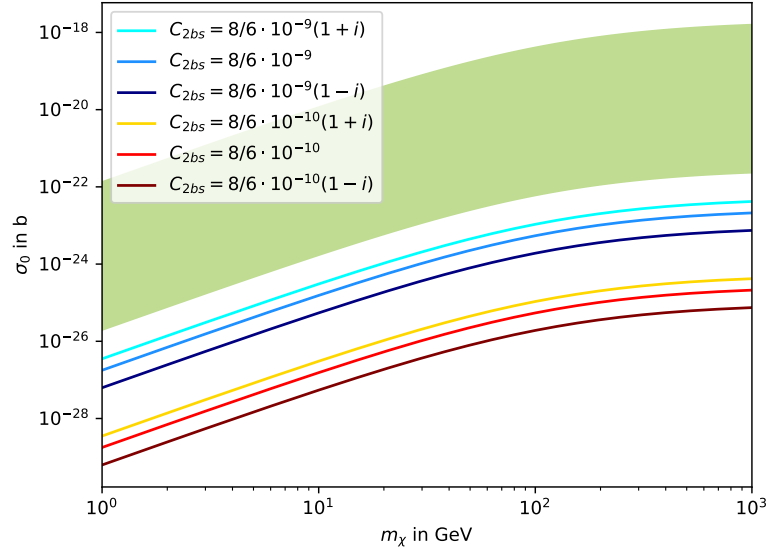
Second, we focus on the relic density condition in equation (4.2). To that end, we set  $m_{Z'} = 2m_\chi$ , but allow for a 30 % tolerance. For  $q_\chi = 1$ , we set  $g'$  to the lower bound in (4.4):  $g' = 2 \cdot 10^{-3}$ , and for  $q_\chi = 1/6$ , we guess  $g' = 10^{-2}$ . Figure 5.4 shows the corresponding loop cross section again as a green shaded area. Regarding the tree level cross section, we choose  $C_{2bs}$  in strong accordance with (5.1). We find that there are regions for  $m_\chi$  where the tree level cross section reaches the loop cross section. The shaded lines show the lower bound of these regions. At the lower boundary of the green area  $m_{Z'} = 2m_\chi \cdot 1.3$ . The tables 5.1 and 5.2 show the obtained lower bounds (l. b.) for the dark matter mass, the resulting values for the  $Z'$  mass, and the ratio of the  $Z'$  mass and the coupling  $g'$ . The ratios are clearly far from being within the bounds of equation (4.1) and thus, the region where flavour mixing becomes relevant cannot address the  $B \rightarrow K\bar{l}l$  discrepancies.

**Table 5.1:**  $q_\chi = 1$ . Bounds for dark matter and  $Z'$  masses (in GeV) and ratio  $m_{Z'}/g'$  (in GeV).

$C_{2bs}$ in $\text{GeV}^{-2}$	l. b. for $m_\chi$	$m_{Z'}$	$m_{Z'}/g'$
$8 \cdot 10^{-10}$	22	57	$29 \cdot 10^3$
$8 \cdot 10^{-10}(1+i)$	18	48	$24 \cdot 10^3$
$3 \cdot 10^{-9}$	11	29	$15 \cdot 10^3$

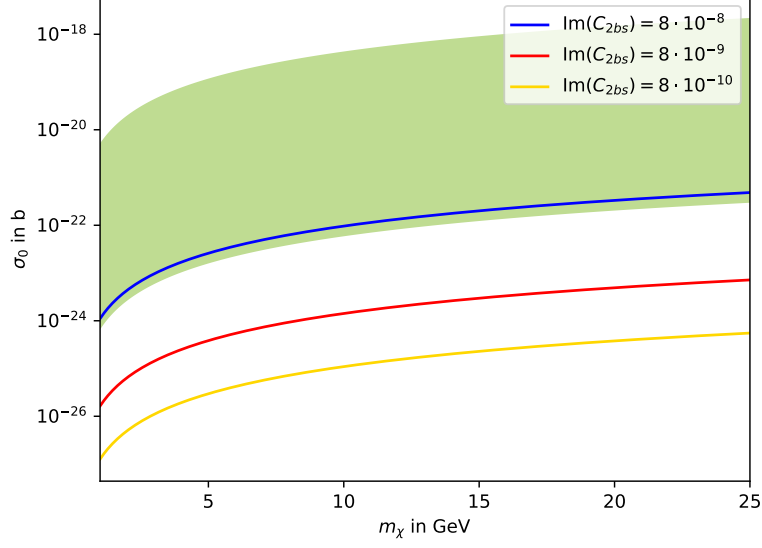
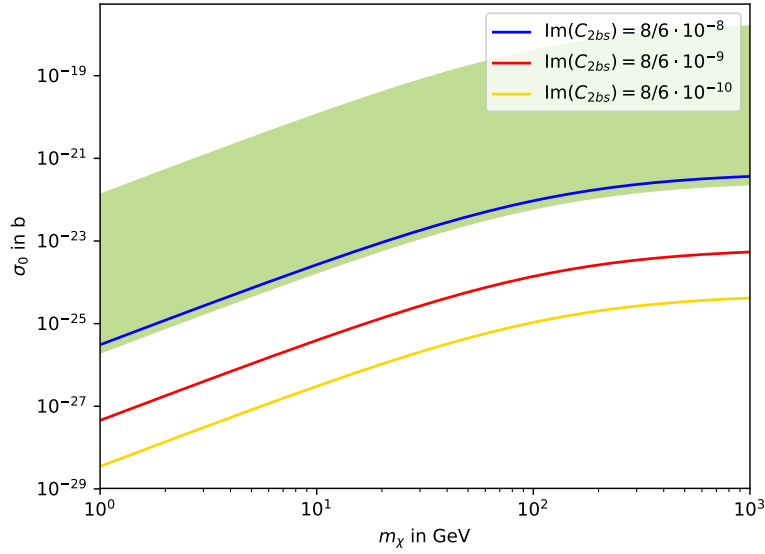
**Table 5.2:**  $q_\chi = 1/6$ . Bounds for dark matter and  $Z'$  masses (in GeV) and ratio  $m_{Z'}/g'$  (in GeV).

$C_{2bs}$ in $\text{GeV}^{-2}$	l. b. for $m_\chi$	$m_{Z'}$	$m_{Z'}/g'$
$1/6 \cdot 8 \cdot 10^{-10}$	108	281	$28 \cdot 10^3$
$1/6 \cdot 8 \cdot 10^{-10}(1+i)$	91	237	$24 \cdot 10^3$
$1/6 \cdot 3 \cdot 10^{-9}$	56	146	$15 \cdot 10^3$

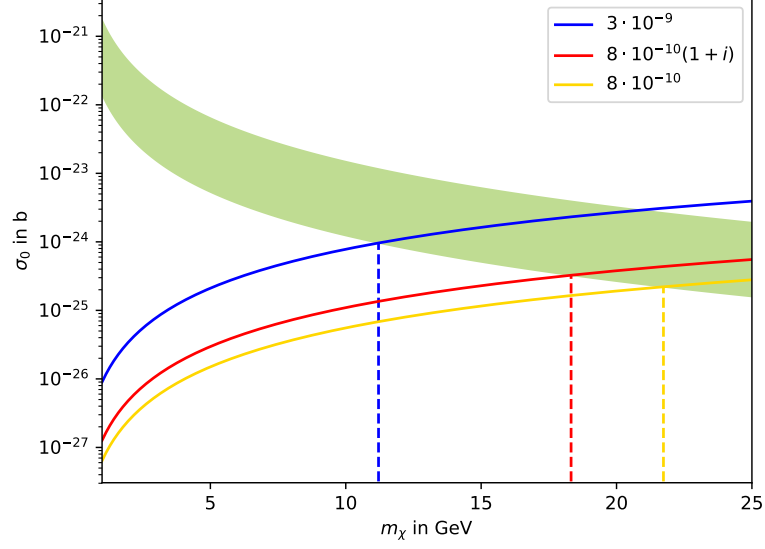

 (a)  $q_l = q_\chi = 1$ 

 (b)  $q_l = 1, q_\chi = 1/6$ 

**Figure 5.2:** Comparison of nucleon cross sections with focus on the bound in equation (4.1) that addresses anomalies in  $B \rightarrow K\bar{l}l$ . The shaded green area represents  $\sigma_{0,\text{loop}}$  with the bounds in (4.1). The coloured lines show  $\sigma_{0,\text{tree}}$  for different values of  $C_{2bs}$  (in  $\text{GeV}^{-2}$ ).

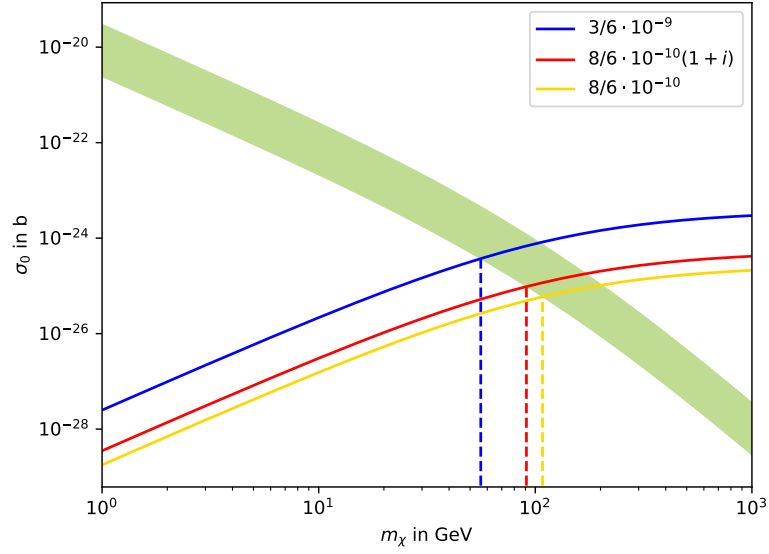


(a)  $q_l = q_\chi = 1$ (b)  $q_l = 1, q_\chi = 1/6$ 

**Figure 5.3:** Like 5.2, but the real part of  $C_{2bs}$  is fixed at  $8 \cdot 10^{-10} \text{ GeV}^{-2}$  and only  $\text{Im}(C_{2bs})$  is varied.



(a)  $q_l = q_\chi = 1, g' = 2 \cdot 10^{-3}$



(b)  $q_l = 1, q_\chi = 1/6, g' = 10^{-2}$

**Figure 5.4:** Comparison of nucleon cross sections with focus on the bound in equation (4.2) that produces the right relic density. The shaded green area represents the loop cross section  $\sigma_{0,\text{loop}}$  at fixed coupling constant  $g'$  and  $m_{Z'} = 2m_\chi$  with a  $\pm 30\%$  tolerance.

To summarize, if we respect the given bounds of the  $B \rightarrow K\bar{l}l$  anomalies, we cannot find any parameter configuration for which the flavour mixing becomes relevant. So, Altmannshofer et. al. correctly neglect quark flavour mixing in the nucleus in their discussion in [1]. However, the setup presented in chapter 3 is universal and may be used to ascertain the irrelevance of flavour mixing in other propositions of new physics with a connection to dark matter.



## Bibliography

- [1] W. Altmannshofer, S. Gori, S. Profumo, and F. S. Queiroz. *Explaining Dark Matter and B Decay Anomalies with an  $L_\mu - L_\tau$  Model*. 2017. arXiv: 1609.04026v2 [hep-ph].
- [2] O. Breidbach. *Geschichte der Naturwissenschaften. I: Die Antike*. Springer Spektrum, 2015.
- [3] E. Garrett and G. Duda. *Dark Matter: A Primer*. 2010. arXiv: 1006.2483 [hep-ph].
- [4] D Griffiths. *Introduction to Elementary Particles*. Wiley, 1987.
- [5] M. E. Peskin and D. V. Schroeder. *An Introduction to Quantum Field Theory*. Perseus Books, 1995.
- [6] K. Anikeev et al. *B Physics at the Tevatron: Run II and Beyond*. 2001. arXiv: 0201071 [hep-ph].
- [7] C. Patrignani et al. “Review of Particle Physics”. In: *Chin. Phys.* C40 (2016).
- [8] F. Bishara, J. Brod, B. Grinstein, and J. Zupan. *Chiral Effective Theory of Dark Matter Direct Detection*. 2017. arXiv: 1611.00368v3 [hep-ph].
- [9] W. Altmannshofer, S. Gori, M. Pospelov, and I. Yavin. *Dressing  $L_\mu - L_\tau$  in Color*. 2016. arXiv: 1403.1269v3 [hep-ph].
- [10] G. Jungman, M. Kamionkowski, and K. Griest. “Supersymmetric dark matter”. In: *Physics Reports* 267 (Mar. 1996).
- [11] T. Marrodan Undagoitia and L. Rauch. *Dark matter direct-detection experiments*. 2017. arXiv: 1509.08767 [physics.ins-det].



## Eidesstattliche Versicherung

Ich versichere hiermit an Eides statt, dass ich die vorliegende Abschlussarbeit mit dem Titel “Flavour Mixing Effects in the Direct Detection of Dark Matter” selbstständig und ohne unzulässige fremde Hilfe erbracht habe. Ich habe keine anderen als die angegebenen Quellen und Hilfsmittel benutzt, sowie wörtliche und sinngemäße Zitate kenntlich gemacht. Die Arbeit hat in gleicher oder ähnlicher Form noch keiner Prüfungsbehörde vorgelegen.

---

Ort, Datum

---

Unterschrift

## Belehrung

Wer vorsätzlich gegen eine die Täuschung über Prüfungsleistungen betreffende Regelung einer Hochschulprüfungsordnung verstößt, handelt ordnungswidrig. Die Ordnungswidrigkeit kann mit einer Geldbuße von bis zu 50 000 € geahndet werden. Zuständige Verwaltungsbehörde für die Verfolgung und Ahndung von Ordnungswidrigkeiten ist der Kanzler/die Kanzlerin der Technischen Universität Dortmund. Im Falle eines mehrfachen oder sonstigen schwerwiegenden Täuschungsversuches kann der Prüfling zudem exmatrikuliert werden (§ 63 Abs. 5 Hochschulgesetz –HG–).

Die Abgabe einer falschen Versicherung an Eides statt wird mit Freiheitsstrafe bis zu 3 Jahren oder mit Geldstrafe bestraft.

Die Technische Universität Dortmund wird ggf. elektronische Vergleichswerkzeuge (wie z. B. die Software “turnitin”) zur Überprüfung von Ordnungswidrigkeiten in Prüfungsverfahren nutzen.

Die oben stehende Belehrung habe ich zur Kenntnis genommen.

---

Ort, Datum

---

Unterschrift